

Numerical Simulation of Rock Burst of Circular Roadway Based on RFPA Software

Yanbo Zhang ^{1,a}, Jian Li¹, Baozhu Tian¹

¹*School of Mining Engineering of North China University of Science and Technology, Tangshan, Hebei, China*

Abstract. Based on RFPA software, the numerical simulation of rock burst in circular roadway is carried out under different horizontal stresses. The paper studies the distribution of stress field, the crack propagation and acoustic emission characteristics in the process of rock burst. The results show that the stress moves and the concentration of compressive stress appears on left and right sides of roadway after excavation of the roadway, and tensile stress zone appears at the top and bottom of the roadway. The shear fracture on the roadway's left and right sides is more serious. The larger the horizontal stress is, the earlier the energy releases and the higher the total energy is.

1 INTRODUCTION

The world's oldest rock burst occurs in Britain in 1738. So far, rock burst has happened in more than 20 countries, such as South Africa, Canada, Japan, Britain, India, China and so on [1]. Many scholars generally hold the thought that rock burst is a kind of dynamic disaster, and due to underground excavation under the condition of high ground stress, the stress redistribution, the elastic energy stored in rock mass suddenly releases, which results in the rock blowout, loose, particle ejection and even throwing damage[2]. As many mines develop to deep area, the frequency of rock burst increases. The rock burst will threaten the safety of builder and equipments, causing a huge loss to produce. Rock burst has become one of worldwide problems of underground rock engineering.

In order to study the breeding rule of rock burst, people use various means to monitor the occurrence of rock burst, such as acoustic emission, microseismic and infrared radiation and so on. However the study on crack evolution process of rock burst is little. Numerical simulation technology has become an important method to research rock burst. In the literature[3], the instability and rupture of rock in unloading process reappears with RFPA2D, and the mechanism of rock burst is discussed. The literature[4] simulates the excavation process of rock cavern with numerical method, and analyze the release of elastic energy of rock burst. The literature[5] simulates the rock burst of circular roadway under the condition of unloading process with RFPA. In the literature[6], the instability rupture of deep roadway caused by dynamic disturbance is simulated, and the mechanism of rock burst triggered by dynamic disturbance is revealed.

The biggest advantage of RFPA^{2D} software compared with other numerical software is the ability to

use homogeneous degree m -value to reflect the homogeneity of material in the numerical model. The majority of mines with occurrence of rock burst are granites. Based on this, aiming at the physical and mechanical performance of granite sample, this paper uses RFPA^{2D} to simulate rock burst of excavation process of roadway under different horizontal stresses. The distribution of stress field, crack extension and acoustic emission(AE) characteristics in the process of rock burst are analyzed, attempting to provide theoretical basis for the study of rock burst.

2 The NUMERICAL MODEL

RFPA^{2D} is used to simulate rock burst induced by excavation of circular roadway with biaxial stress. The partitioning grid of numerical model is 150×150 units, and the hole with diameter of 45 mm is drilled in center when excavating. The model is shown in figure 1.

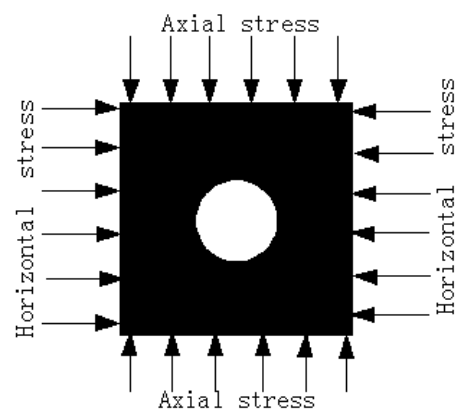


Fig.1 Geometry characteristics of model

^a Corresponding author: lijian19890909@163.com

The parameters of numerical model are selected according to the physical and mechanical parameters of granite with uniaxial loading. Assuming that sample's inhomogeneous mesoscopic unit obeys Weibull distribution. The corresponding parameters are shown in table 1.

Table 1 The distribution parameters of RFPA numerical simulation

Lithology	Homogeneous coefficient	The mean elasticity modulus/MPa	Uniaxial compressive strength/	Poisson ratio	Compression tension
granite	3	60000	140	0.25	10

The model is biaxial loading. Three kinds of horizontal stress are set as 9 MPa, 13 MPa, 17 MPa. Firstly, horizontal stress loads to the preset value. Then the axial stress loads step by step and the displacement increment of each step is 0.005 mm. When loading to the original rock stress, the roadway is excavated. In the simulation, when axial stress loads to 40 MPa, excavate roadway and axial stress continues loading to the occurrence of rock burst.

3 The RESULTS OF NUMERICAL SIMULATION

The damage forms of rock burst triggered by roadway excavation under three different horizontal stresses are similar. The transfixion cracks both appear on left and right sides of roadway with 45° to the vertical direction. Limited to the space, the numerical simulation result of horizontal stress 9 MPa is only shown in figure 2. The higher the brightness in the maximum principal stress diagram is, the larger the primitive stress is. It is found that before excavation of roadway, the stress distribution is uniform. In the 20th step, after excavation of roadway, the stress state of equilibrium is broken, and stress field near the roadway adjusts. The compressive stress concentration appears on left and right sides of roadway, and tensile stress zone appears at the top and bottom of roadway. When the stress achieves ultimate strength of materials, the micro cracks begin to appear surrounding the roadway. Then micro rupture first appears in two sides of roadway and at the top and bottom of roadway is tiny tensile crack.

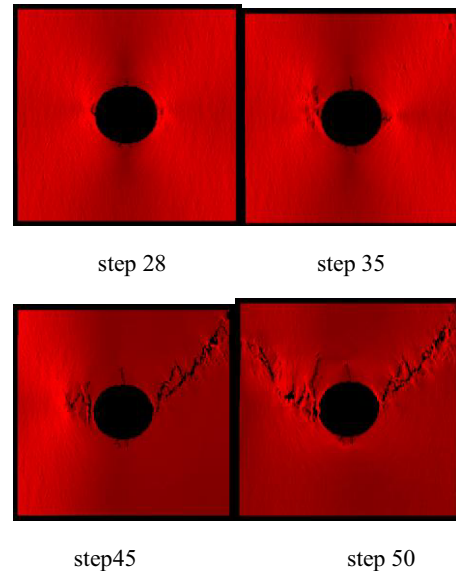
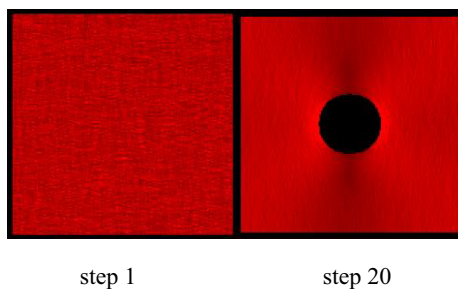


Fig.2 The maximum principal stress diagrams with horizontal stress 9 MPa

In the initial stage, the micro fracture is distributed on left and right sides of roadway in isolation, and no obvious interaction between micro fractures. As load increases, the phenomenon of fracture cluster becomes more and more intense, and the element brightness of crack tip becomes higher. The new stress concentration zone forms in deep surrounding rock, and the cracks extend along the stress concentration zone from both edge of left and right sides of the roadway to deep surrounding rock. As the vertical deformation increases, the cracks extend upwards. Since then, random and independent cracks appear at 45° to the vertical direction. Due to the increasing of remote cracks, finally the ruptured units interconnect and extend to the boundary of sample, forming penetrating crack and leading to macroscopic damage. The roadway becomes out of shape. The lateral pressure coefficient is less than 1, so the shear failure with compressive stress concentration on left and right sides of roadway is more serious, and tensile failure at the top and bottom of the roadway develops slowly.

The main reason causing macro damage isn't the tensile crack at the top and bottom of the roadway, but the weakening bands with 45° to the direction of maximum principal stress. The shear slip in weakening bands make the no damage parts appear torsional shear and connection, forming the macroscopic zone of fracture. Brittle fracture occurs and triggers rock burst.

The diagrams of AE energy rate-total AE energy-time are shown in figure 3. The excavation of roadway occurs in the 20th step. It can be seen that no energy releases before excavation of roadway and energy releases after excavation. When horizontal stress is 9 MPa, energy release first appears in the 31th step and total energy release is 0.113J; When horizontal stress is 13 MPa, energy release first appears in the 29th step and total energy release is 0.151J; When horizontal stress is 17 MPa, energy release first appears in the 26th step and total energy release is 0.177J. It can be found that the larger the horizontal stress is, the earlier the energy releases, and the higher the total energy releases. It indicates that the deeper the burial depth is and the larger the horizontal stress is, the higher the accumulative

energy of rock mass is. Due to disturbance of excavation, the energy releases earlier and higher. It is more prone to trigger severe rock burst.

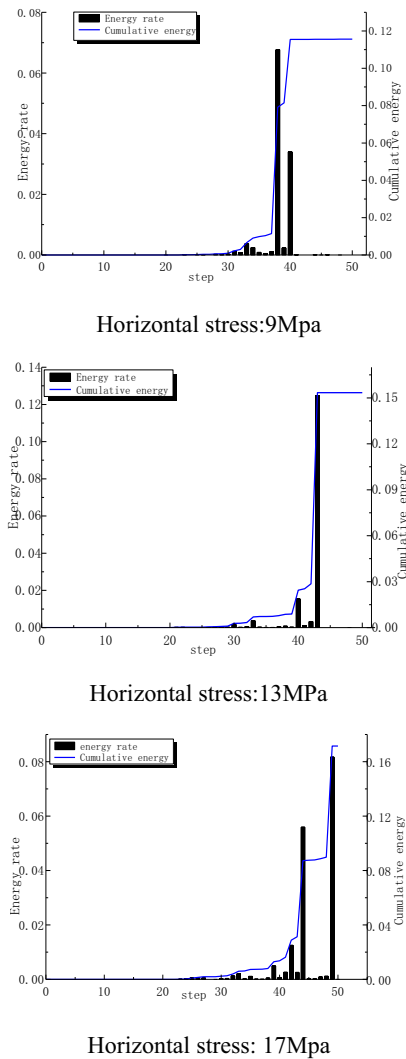


Fig. 3 The diagrams of AE energy rate-total AE energy-time are shown

In low stress state, the rock burst mainly occurs with tensile failure and shear failure is auxiliary. While in high stress state, the rock burst mainly occurs with shear failure, extending with shear failure modes from left and right sides of roadway to deep surrounding rock. The main source of energy release is shear fracture, and energy release with tensile fracture is less[7]. So in high horizontal stress, the release of energy is larger and the intensity of rock burst is severer.

4 CONCLUSIONS

RFP software is used to simulating rock burst of roadway under different horizontal stresses. The distribution of stress field and the characteristics of energy release are analyzed. The following conclusions are obtained:

(1) After excavation of roadway, the stress field adjusts. The compressive stress concentration appears on left and right sides of the roadway, and the tensile stress zone appears at the top and bottom of the roadway.

(2) The lateral pressure coefficient is less than 1, so the shear failure with compressive stress concentration on left and right sides of roadway is more serious, and tensile failure at the top and bottom of the roadway develops slowly.

(3) The horizontal stress increases, then shear failure increases in the process of rock burst. The deeper the burial depth is and the larger the horizontal stress is, the earlier and higher the energy releases. It is more prone to trigger rock burst.

Acknowledgments

The national natural science foundation of China(51374088,51174071), the natural science foundation of Hebei Province(E2012209047).

References

1. Blake, Wilson. Rockbursts: Case studies from North American Hard-Rock mines[M]. Society for Mining Metallurgy & Exploration, 2004, 3.
 2. Manchao HE, Jinli MIAO, Dejian LI, et al. Experimental study of rock burst of granite in deep mine. Chinese Journal of Rock Mechanics and Engineering, 2007, 05:865-876. (In Chinese)
 3. Zhiping HUANG, Chun'an TANG, Tianhui MA, et al. Chinese Journal of Rock Mechanics and Engineering, 2011, S1:3120-3128. (In Chinese)
 4. Yaohui WANG. Rock and Soil Mechanics, 2008, 03: 790-794. (In Chinese)
 5. Jinshan SUN, Qihu ZHU, Wenbo LU. Journal of China University of Mining & Technology, 2007(17)4:552-556. (In Chinese)
 6. Wancheng ZHU, Chun'an TANG, Tianhong YANG, et al. Chinese Journal of Rock Mechanics and Engineering, 2003, 22(1):24-29. (In Chinese)
 7. Qingqing JIANG, Jiangteng LI, Yifu HU, et al. Rock and Soil Mechanics, 2008, 29(9):2527-2530. (In Chinese)
- A. Mecke, I. Lee, J.R. Baker jr., M.M. Banaszak Holl, B.G. Orr, Eur. Phys. J. E 14, 7 (2004)